Figure S1, related to Figures 1 and 2

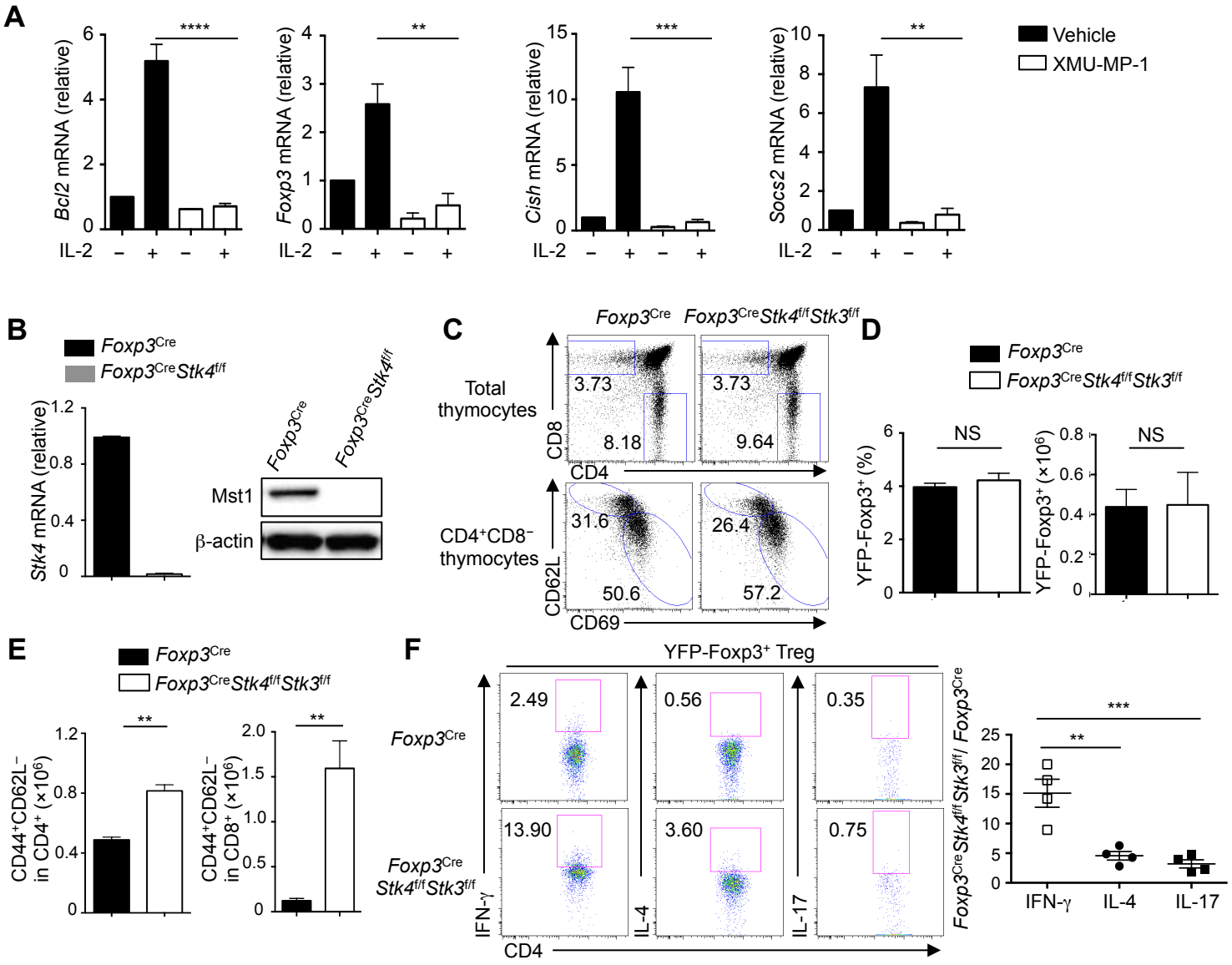

Figure S1, related to Figures 1 and 2. Mst1 mediates IL-2 signaling and deletion of Mst1−Mst2 in Tregs disrupts immune homeostasis but not thymic development. (A) CD4$^+$CD25$^+$ Tregs were stimulated with IL-2 (5 U/ml) for 12 h, in the presence of vehicle or the Mst1 inhibitor XMU-MP-1 (5 μM), and the mRNA expression of *Bcl2, Foxp3, Cish,* and *Socs2* was analyzed by real-time PCR (n = 3). (B) Analysis of Mst1 mRNA (*Stk4*; left) and protein (right) expression in YFP$^+$ Tregs from *Foxp3*^{Cre} and *Foxp3*^{Cre}*Stk4*$^{f/f}$ mice. (C) Flow cytometry analysis of CD4 and CD8 expression in total thymocytes (upper) and CD62L and CD69 expression on thymic CD4$^+$CD8$^-$ cells (lower) of 1-month-old *Foxp3*^{Cre} and *Foxp3*^{Cre}*Stk4*$^{f/f}$*Stk3*$^{f/f}$ mice. (D) YFP$^+$ Treg frequency in CD4$^+$CD8$^-$TCRβ$^+$ T cells and number in the thymus of 1-month-old *Foxp3*^{Cre} and *Foxp3*^{Cre}*Stk4*$^{f/f}$*Stk3*$^{f/f}$ mice (n = 5). (E) Numbers of CD44$^+$CD62L$^-$ cells in splenic CD4$^+$ and CD8$^+$ T cells of 1.5-month-old *Foxp3*^{Cre} and *Foxp3*^{Cre}*Stk4*$^{f/f}$*Stk3*$^{f/f}$ mice (n = 4). (F) Flow cytometry analysis of IFN-γ, IL-4 and IL-17 expression in Foxp3$^+$ Tregs in the spleen of 1.5-month-old *Foxp3*^{Cre} and *Foxp3*^{Cre}*Stk4*$^{f/f}$*Stk3*$^{f/f}$ mice (left). Right, fold changes of IFN-γ, IL-4 and IL-17 expression in splenic CD4$^+$ T cells of *Foxp3*^{Cre}*Stk4*$^{f/f}$*Stk3*$^{f/f}$ vs. *Foxp3*^{Cre} mice (n = 4). Numbers in gates indicate percentage of cells. Data in plots indicate means ± s.e.m. NS, not significant; $^{**}P < 0.01$, $^{***}P < 0.001$, $^{****}P < 0.0001$; two-tailed unpaired Student's t test (D, E) or one-way ANOVA (A, F). Data are representative of at least 3 independent experiments (B, C, F) or pooled from at least 3 independent experiments (A, D, E).

Figure S2, related to Figure 2

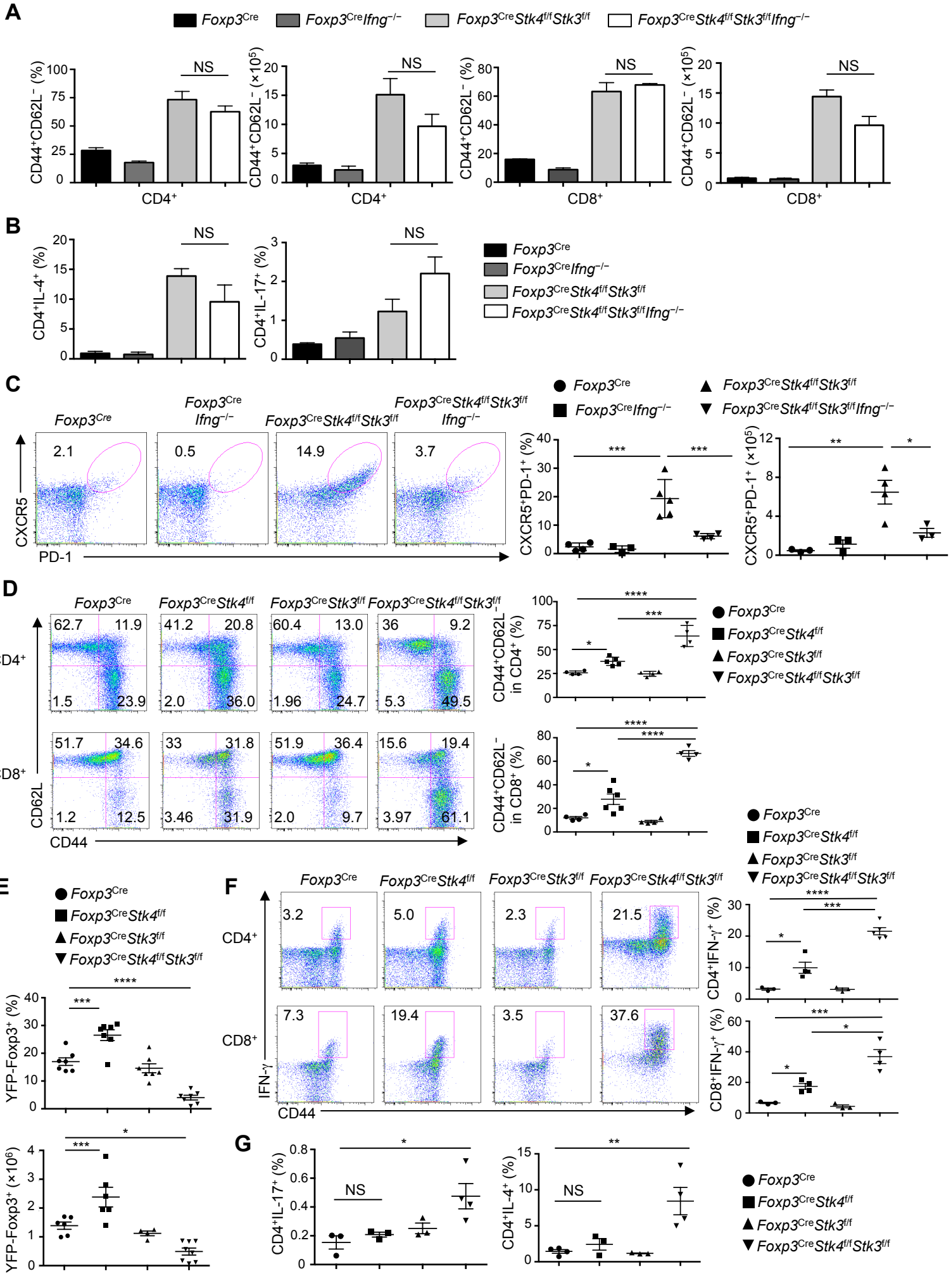

Figure S2, related to Figure 2. IFN-γ is not responsible for driving autoimmunity in *Foxp3*^{Cre}*Stk4*$^{f/f}$*Stk3*$^{f/f}$ mice, and Mst1 plays a dominant role over Mst2 in regulating Treg function. (A) Frequency and number of CD44^{+}CD62L^{-} population in splenic CD4^{+} or CD8^{+} T cells of 1.5-month-old *Foxp3*^{Cre}, *Foxp3*^{Cre}*Ifng*$^{-/-}$, *Foxp3*^{Cre}*Stk4*$^{f/f}$*Stk3*$^{f/f}$ and *Foxp3*^{Cre}*Stk4*$^{f/f}$*Stk3*$^{f/f}$*Ifng*$^{-/-}$ mice (n = 3). (B) Frequencies of splenic IL-4^{+} and IL-17^{+} populations in CD4^{+} T cells of 1.5-month-old *Foxp3*^{Cre}, *Foxp3*^{Cre}*Ifng*$^{-/-}$, *Foxp3*^{Cre}*Stk4*$^{f/f}$*Stk3*$^{f/f}$ and *Foxp3*^{Cre}*Stk4*$^{f/f}$*Stk3*$^{f/f}$*Ifng*$^{-/-}$ mice (n = 3). (C) Flow cytometry analysis (left) and quantification of frequency and number (right) of Tfh cells (CD4^{+}B220^{-}CXCR5^{+}PD-1^{+}) in the spleen of 1.5-month-old *Foxp3*^{Cre}, *Foxp3*^{Cre}*Ifng*$^{-/-}$, *Foxp3*^{Cre}*Stk4*$^{f/f}$*Stk3*$^{f/f}$ and *Foxp3*^{Cre}*Stk4*$^{f/f}$*Stk3*$^{f/f}$*Ifng*$^{-/-}$ mice ($n \geq 3$). (D) Flow cytometry analysis of CD62L and CD44 expression on splenic CD4^{+} T cells of 1.5-month-old *Foxp3*^{Cre}, *Foxp3*^{Cre}*Stk4*$^{f/f}$, *Foxp3*^{Cre}*Stk3*$^{f/f}$, and *Foxp3*^{Cre}*Stk4*$^{f/f}$*Stk3*$^{f/f}$ mice (left). Right, frequency of CD44^{+}CD62L^{-} population in CD4^{+} or CD8^{+} T cells ($n \geq 4$). (E) YFP^{+} Treg frequency and number in splenic CD4^{+} T cells of 1.5-month-old *Foxp3*^{Cre}, *Foxp3*^{Cre}*Stk4*$^{f/f}$, *Foxp3*^{Cre}*Stk3*$^{f/f}$, and *Foxp3*^{Cre}*Stk4*$^{f/f}$*Stk3*$^{f/f}$ mice ($n \geq 4$). (F) Flow cytometry analysis of IFN-γ and CD44 expression in splenic CD4^{+} and CD8^{+} T cells of 1.5-month-old *Foxp3*^{Cre}, *Foxp3*^{Cre}*Stk4*$^{f/f}$, *Foxp3*^{Cre}*Stk3*$^{f/f}$, and *Foxp3*^{Cre}*Stk4*$^{f/f}$*Stk3*$^{f/f}$ mice (left). Right, frequencies of IFN-γ^{+} CD4^{+} and CD8^{+} T cells ($n \geq 3$). (G) Frequencies of IL-17^{+} and IL-4^{+} populations in splenic CD4^{+} T cells of 1.5-month-old *Foxp3*^{Cre}, *Foxp3*^{Cre}*Stk4*$^{f/f}$, *Foxp3*^{Cre}*Stk3*$^{f/f}$ and *Foxp3*^{Cre}*Stk4*$^{f/f}$*Stk3*$^{f/f}$ mice ($n \geq 3$). Numbers in quadrants or gates indicate percentage of cells. Data in plots indicate means ± s.e.m. NS, not significant; **P* < 0.05, ***P* < 0.01, ****P* < 0.001; one-way ANOVA (A–G). Data are pooled from at least 3 independent experiments (A, B, E, G) or representative of at least 3 independent experiments (C, D, F).

Figure S3, related to Figure 3

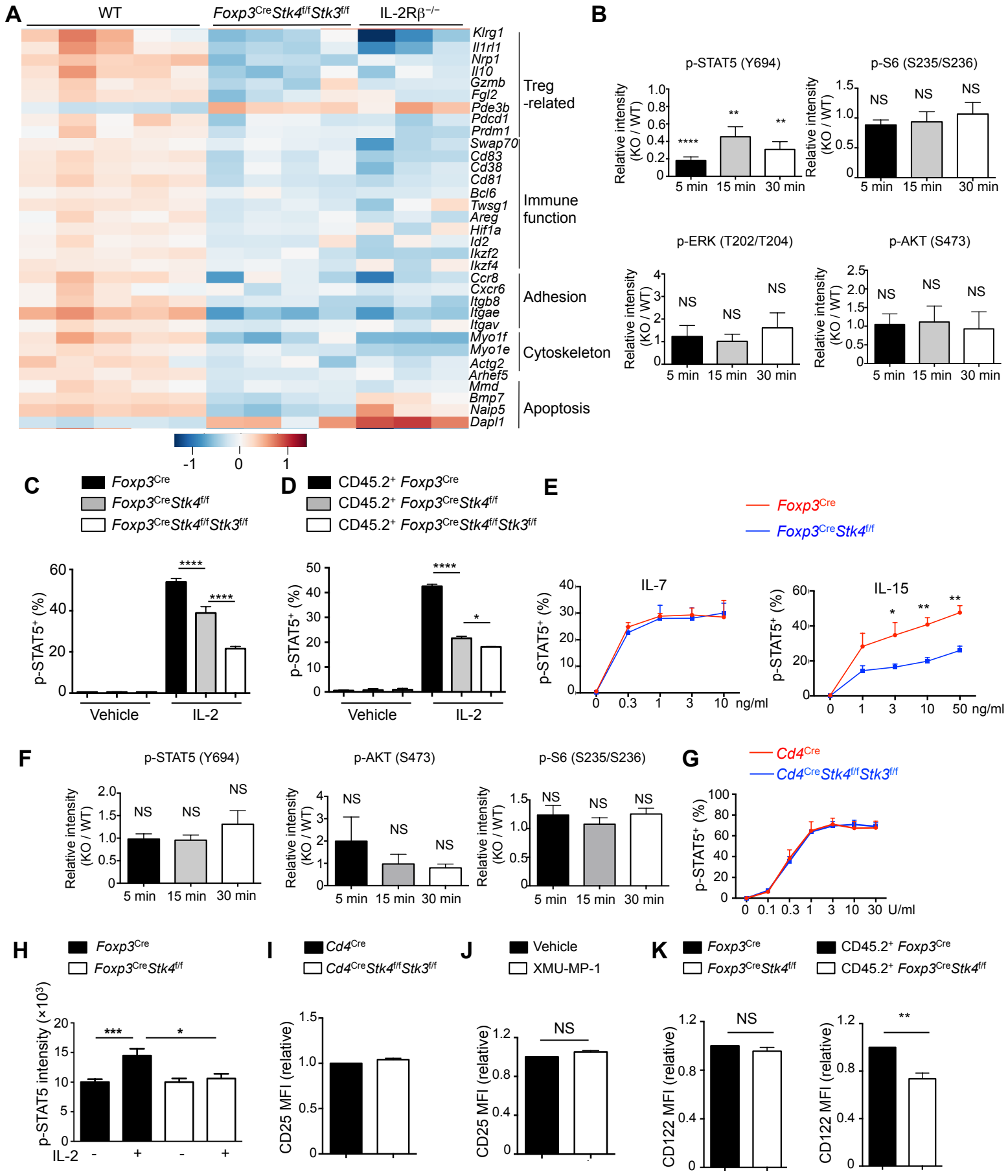

Figure S3, related to Figure 3. Mst1−Mst2-deficient Tregs have altered gene expression and IL-2R signaling. (A) Heat map showing gene expression changes in Mst1−Mst2-deficient and IL-2Rβ-deficient Tregs. (B) Statistics of immunoblot analysis (Figure 3F) of p-STAT5 (Y694), p-S6 (S235/S236), p-ERK (T202/T204) and p-AKT (S473) in Mst1-deficient (KO) vs. WT Tregs upon IL-2 stimulation for the indicated time points (n = 3). (C) YFP$^+$ Tregs were isolated from age-matched 1.5-month-old *Foxp3*^{Cre}, *Foxp3*^{Cre}*Stk4*$^{f/f}$ and *Foxp3*^{Cre}*Stk4*$^{f/f}$*Stk3*$^{f/f}$ mice (n = 3) and stimulated with 1 U/ml IL-2 for 30 min for p-STAT5 analysis by flow cytometry. The p-STAT5$^+$ Treg frequency was quantified. (D) CD45.2$^+$YFP$^+$ Tregs from mixed BM chimeric *Foxp3*^{Cre}, *Foxp3*^{Cre}*Stk4*$^{f/f}$ and *Foxp3*^{Cre}*Stk4*$^{f/f}$*Stk3*$^{f/f}$ mice (n = 3) were stimulated with 1 U/ml IL-2 for 30 min for p-STAT5 analysis by flow cytometry. The p-STAT5$^+$ Treg frequency was quantified. (E) Statistics of p-STAT5$^+$ Treg frequency in WT or Mst1-deficient Tregs (n = 3) stimulated with IL-7 or IL-15 for 30 min. (F) Statistics of immunoblot analysis (Figure 3G) of p-STAT5 (Y694), p-AKT (S473) and p-S6 (S235/S236) in Mst1−Mst2-deficient (KO) vs. WT activated T cell blasts upon IL-2 stimulation (n = 3). (G) T cell blasts were rested without IL-2 for 8 h at 37ºC followed by IL-2 stimulation for 30 min and analyzed for p-STAT5 by flow cytometry (n = 3). The p-STAT5$^+$ cell frequency was quantified. (H) Statistics of nuclear p-STAT5 immunofluorescence signal in WT and Mst1-deficient Tregs in response to 1 U/ml IL-2 stimulation for 0 and 30 min (n > 20). (I) Statistics of CD25 expression on WT or Mst1−Mst2-deficient CD4$^+$ T cell blasts (n = 3) after anti-CD3-CD28 stimulation for 3 days and rested for another 3 days. CD25 MFI in WT CD4$^+$ T cell blasts was normalized to 1 in statistics. (J) Freshly isolated WT CD4$^+$CD25$^+$ Tregs were pretreated with vehicle or 5 μM Mst1 inhibitor XMU-MP-1 for 1 h at 37ºC followed by 0-30 U/ml IL-2 stimulation for 30 min (n = 4 per treatment). CD25 expression was examined by flow cytometry after the 1 h vehicle or XMU-MP-1 treatment, with the value in vehicle-treated cells normalized to 1. (K) Left, statistics of flow cytometry analysis of CD122 expression on splenic YFP$^+$ Tregs from *Foxp3*^{Cre} and *Foxp3*^{Cre}*Stk4*$^{f/f}$ mice (n = 3). Right, statistics of flow cytometry analysis of CD122 expression on splenic YFP$^+$ Tregs from mixed BM chimeric *Foxp3*^{Cre} and *Foxp3*^{Cre}*Stk4*$^{f/f}$ mice (n = 3). CD122 MFI in WT Tregs was normalized to 1 in statistics. Data in plots indicate means ± s.e.m. NS, not significant; *P < 0.05, **P < 0.01, ***P < 0.001, ****P < 0.0001; two-tailed unpaired Student's t test (B–F, J, K) or one-way ANOVA (H). Data are from one experiment (A, H) or representative of 3 independent experiments (I) or pooled from at least 3 independent experiments (B–G, J, K).

Figure S4, related to Figure 4

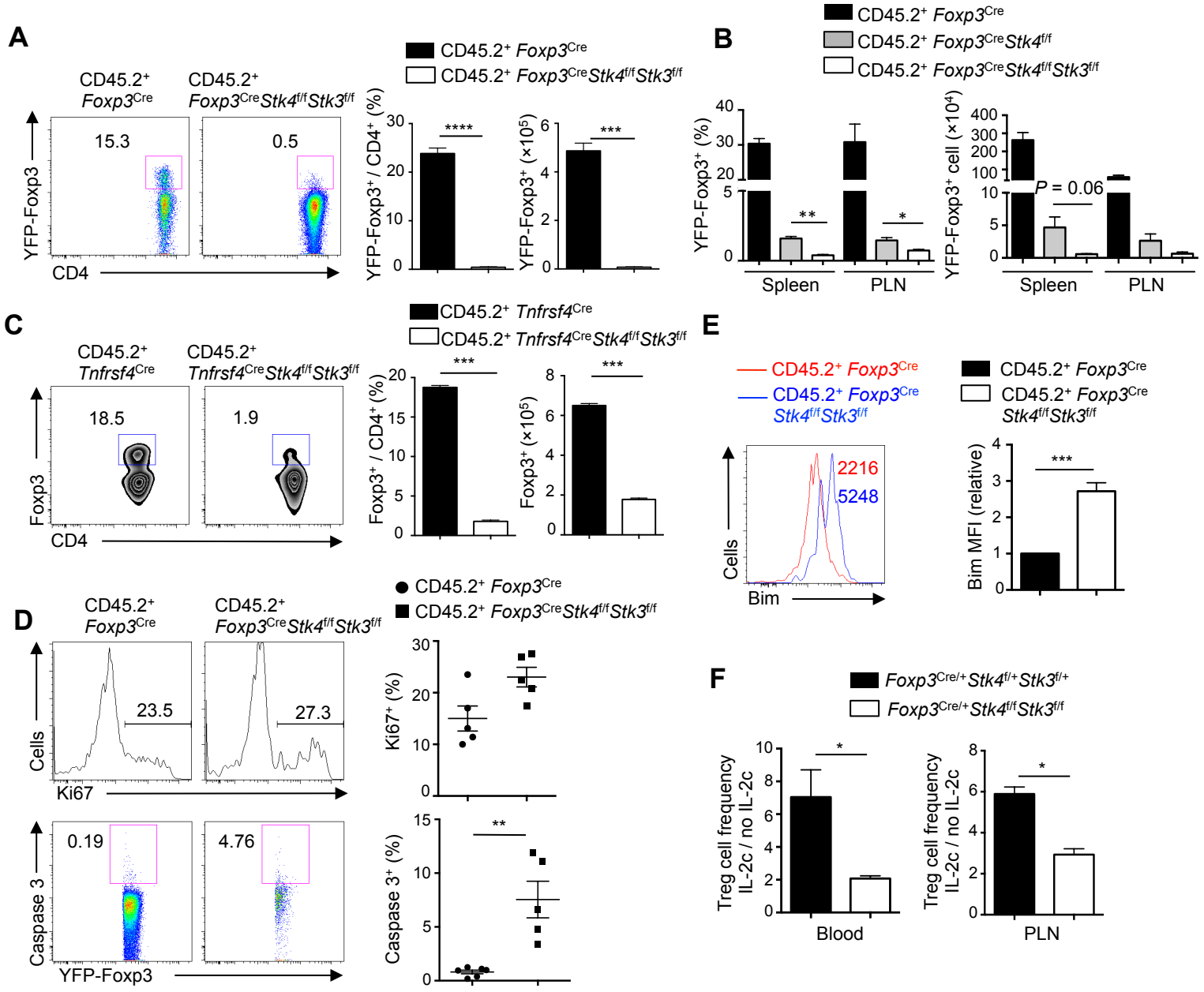

Figure S4, related to Figure 4. Reduced Mst1−Mst2-deficient Treg pool and survival in mixed bone marrow chimeras. (A) Flow cytometry analysis (left) and frequency and number (right) of YFP$^+$ Tregs in the spleen of CD45.2$^+$ *Foxp3*^{Cre} and CD45.2$^+$ *Foxp3*^{Cre}*Stk4*$^{f/f}$*Stk3*$^{f/f}$ mixed BM chimeras (n = 3). (B) YFP$^+$ Treg frequency and number in CD45.2$^+$CD4$^+$ T cells was examined in the spleen and peripheral lymph nodes (PLN) of mixed BM chimeric *Foxp3*^{Cre}, *Foxp3*^{Cre}*Stk4*$^{f/f}$ and *Foxp3*^{Cre}*Stk4*$^{f/f}$*Stk3*$^{f/f}$ mice (n = 3). (C) Flow cytometry analysis (left) and frequency and number (right) of Foxp3$^+$ Tregs in the spleen of CD45.2$^+$ *Tnfrsf4*^{Cre} *and* CD45.2$^+$ *Tnfrsf4*^{Cre}*Stk4*$^{f/f}$*Stk3*$^{f/f}$ mixed BM chimeras (n = 3). (D) Flow cytometry analysis and statistics of Ki67 (upper) and active caspase 3 (lower) expression in YFP$^+$ Tregs in the spleen of CD45.2$^+$ *Foxp3*^{Cre} and CD45.2$^+$ *Foxp3*^{Cre}*Stk4*$^{f/f}$*Stk3*$^{f/f}$ mixed BM chimeras. (E) Flow cytometry analysis and statistics of Bim expression in YFP$^+$ Tregs in the spleen of CD45.2$^+$ *Foxp3*^{Cre} and CD45.2$^+$ *Foxp3*^{Cre}*Stk4*$^{f/f}$*Stk3*$^{f/f}$ mixed BM chimeras. Numbers in graph indicate the MFI. Bim MFI in CD45.2$^+$ *Foxp3*^{Cre} Tregs was normalized to 1 in statistics. (F) As described in Figure 4E, the fold increases of Treg frequency in blood (left) and PLN (right) upon IL-2−α-IL-2 (JES6-1) complex (IL-2c vs. no IL-2c treatment) were presented for WT and Mst1−Mst2-deficient mice (n = 3). Numbers in gates indicate percentage of cells. Data in plots indicate means ± s.e.m. *P < 0.05, **P < 0.01, ***P < 0.001, ****P < 0.0001; two-tailed unpaired Student's t test (A–F). Data are representative of 3 independent experiments (A, C–E) or pooled from at least 2 independent experiments (B, F).

Figure S5, related to Figure 5

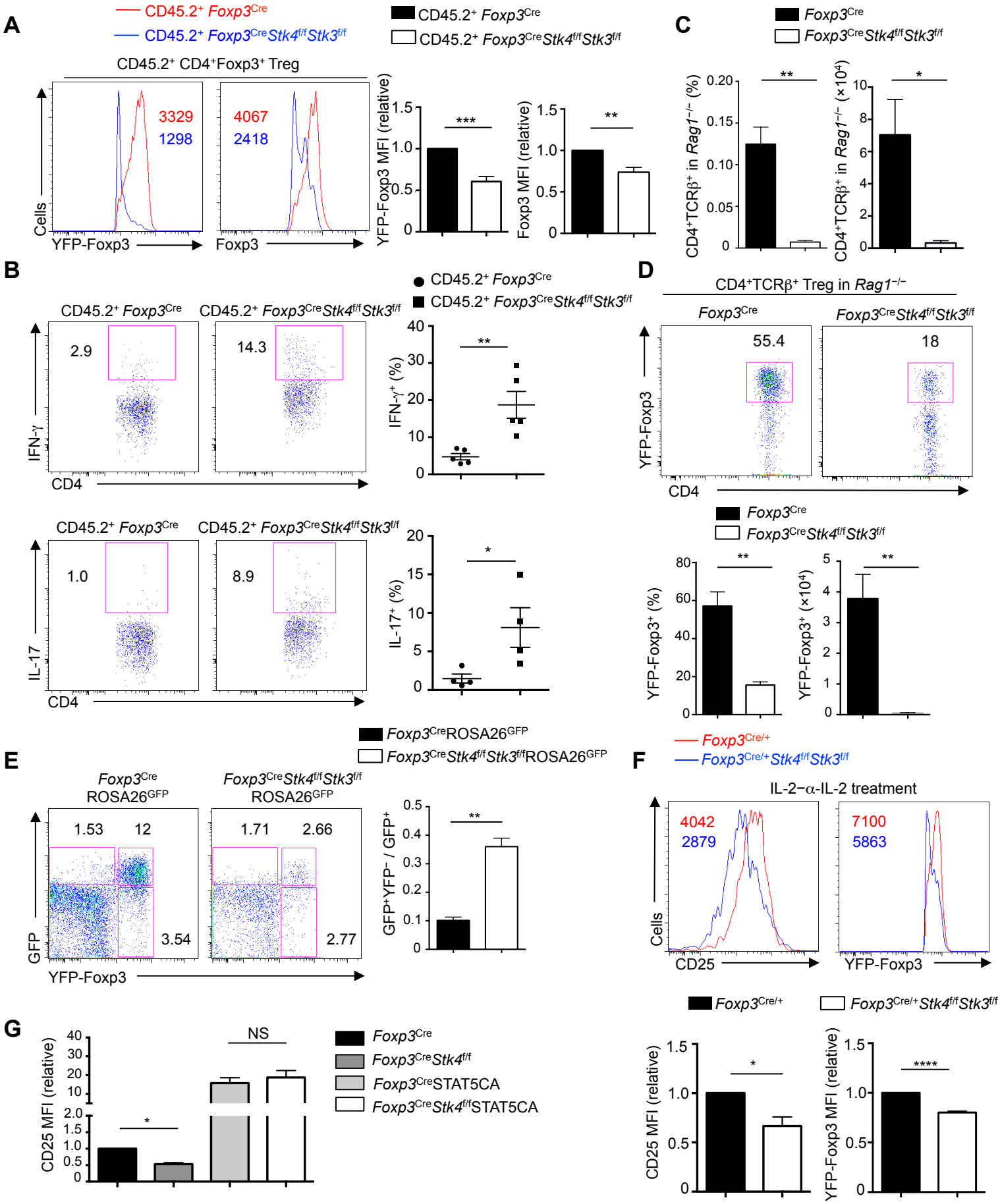

Figure S5, related to Figure 5. Reduced lineage stability in Mst1−Mst2-deficient Tregs. (A) Flow cytometry analysis and statistics of YFP-Foxp3 and intracellular Foxp3 protein expression in splenic CD4$^+$ Tregs of CD45.2$^+$ *Foxp3*^{Cre} and CD45.2$^+$ *Foxp3*^{Cre}*Stk4*$^{f/f}$*Stk3*$^{f/f}$ mixed BM chimeras (n = 4). YFP-Foxp3 and Foxp3 protein MFI in CD45.2$^+$ *Foxp3*^{Cre} Tregs were normalized to 1 in statistics. (B) Flow cytometry analysis and statistics of IFN-γ^+ (upper) and IL-17$^+$ (lower) frequency in splenic Foxp3$^+$CD4$^+$ Tregs of CD45.2$^+$ *Foxp3*^{Cre} and CD45.2$^+$ *Foxp3*^{Cre}*Stk4*$^{f/f}$*Stk3*$^{f/f}$ mixed BM chimeras ($n \geq 4$). (C) YFP$^+$ Tregs from *Foxp3*^{Cre} or *Foxp3*^{Cre}*Stk4*$^{f/f}$*Stk3*$^{f/f}$ mice were adoptively transferred to *Rag1*$^{-/-}$ mice, and the frequency and number of transferred CD4$^+$TCRβ^+ T cells in spleen of *Rag1*$^{-/-}$ mice were analyzed 10 days later (n = 3). (D) YFP$^+$ Tregs from *Foxp3*^{Cre} and *Foxp3*^{Cre} *Stk4*$^{f/f}$*Stk3*$^{f/f}$ mice were adoptively transferred into *Rag1*$^{-/-}$ mice, and YFP$^+$ Tregs were analyzed by flow cytometry 10 days later (upper). Lower, frequency and number of remaining YFP$^+$ Tregs among total Tregs (n = 4). (E) Flow cytometry analysis of GFP and YFP-Foxp3 expression in splenic CD4$^+$ T cells from 2-month-old *Foxp3*^{Cre}ROSA26^{GFP} and *Foxp3*^{Cre}*Stk4*$^{f/f}$*Stk3*$^{f/f}$ROSA26^{GFP} mice (left). Right, relative ratio of GFP$^+$YFP$^-$ (ex-Treg) to total GFP$^+$ (Tregs with GFP$^+$YFP$^+$ and GFP$^+$YFP$^-$) populations (n = 2). (F) Flow cytometry analysis and statistics of CD25 and YFP-Foxp3 expression in YFP$^+$ Tregs of female *Foxp3*$^{Cre/+}$ and *Foxp3*$^{Cre/+}$*Stk4*$^{f/f}$*Stk3*$^{f/f}$ mice (n = 4) after IL-2−α-IL-2 (JES6-1) complex treatment (as in Figure 4E). CD25 and YFP-Foxp3 expression in *Foxp3*$^{Cre/+}$ Tregs was normalized to 1 in statistics. (G) As described in Figure 5I, CD25 expression on transduced Tregs was examined 10 days later. Numbers in graphs indicate the mean fluorescence intensity. Numbers in gates indicate percentage of cells. Data in plots indicate means ± s.e.m. NS, not significant; *P < 0.05, **P < 0.01, ***P < 0.001, ****P < 0.0001; two-tailed unpaired Student's t test (A–G). Data are representative of at least 2 independent experiments (A, B, D–F) or pooled from at least 2 independent experiments (C, G).

Figure S6, related to Figure 6

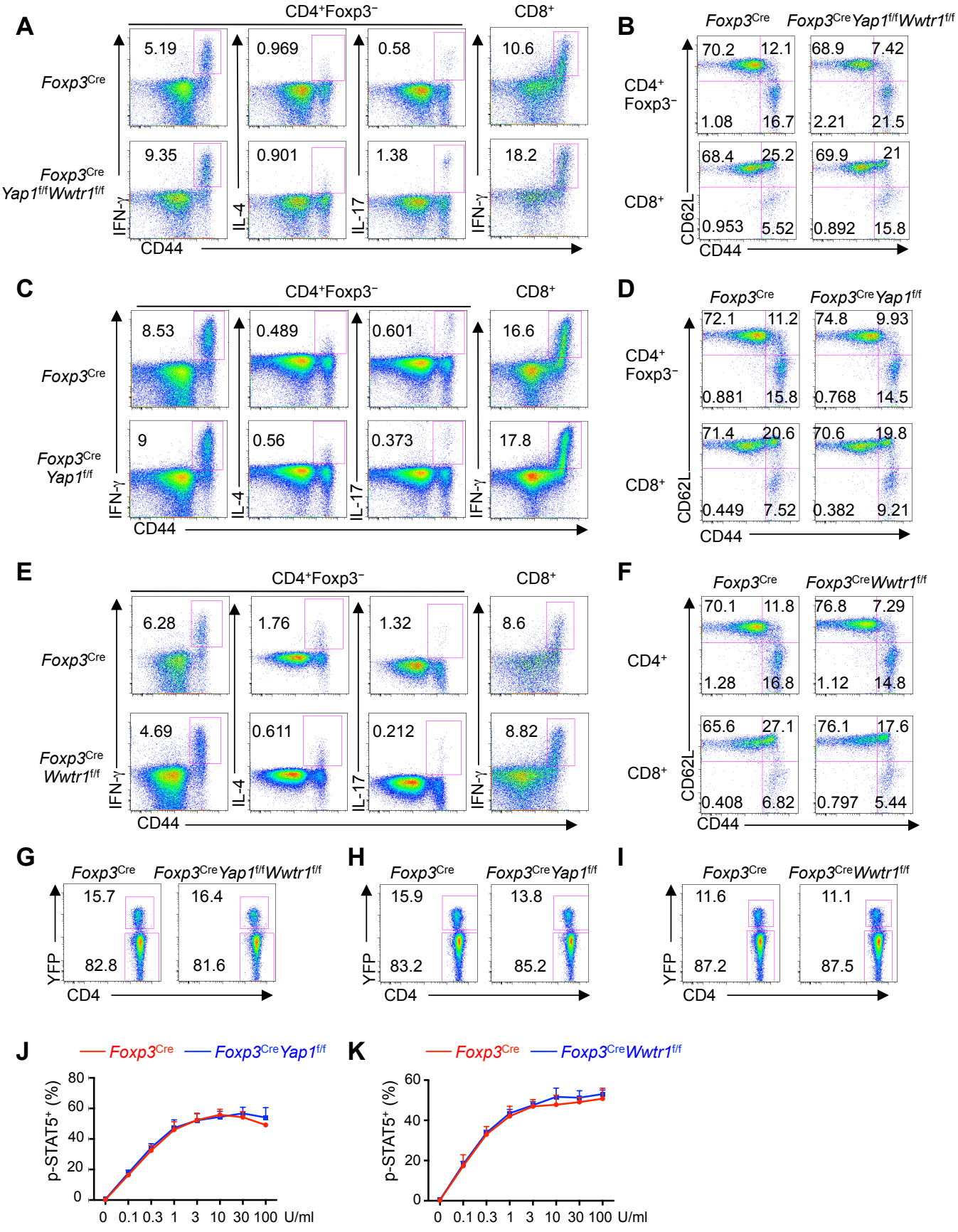

Figure S6, related to Figure 6. Mice with Treg-specific deletion of Yap or Taz have largely normal immune homeostasis. (A) Flow cytometry analysis of IFN-γ, IL-17 and IL-4 expression in splenic $CD4^+Foxp3^-$ T cells and IFN-γ in splenic $CD8^+$ T cells of *Foxp3*^{Cre} and *Foxp3*^{Cre}*Yap1*$^{f/f}$*Wwtr1*$^{f/f}$ mice. (B) Flow cytometry analysis of CD62L and CD44 expression on splenic $CD4^+Foxp3^-$ and $CD8^+$ T cells of *Foxp3*^{Cre} and *Foxp3*^{Cre}*Yap1*$^{f/f}$*Wwtr1*$^{f/f}$ mice. (C) Flow cytometry analysis of IFN-γ, IL-17 and IL-4 expression in splenic $CD4^+Foxp3^-$ T cells and IFN-γ in splenic $CD8^+$ T cells of *Foxp3*^{Cre} and *Foxp3*^{Cre}*Yap1*$^{f/f}$ mice. (D) Flow cytometry analysis of CD62L and CD44 expression on splenic $CD4^+Foxp3^-$ and $CD8^+$ T cells of 6-month-old *Foxp3*^{Cre} and *Foxp3*^{Cre}*Yap1*$^{f/f}$ mice. (E) Flow cytometry analysis of IFN-γ, IL-17 and IL-4 expression in splenic $CD4^+Foxp3^-$ T cells and IFN-γ in splenic $CD8^+$ T cells of *Foxp3*^{Cre} and *Foxp3*^{Cre}*Wwtr1*$^{f/f}$ mice. (F) Flow cytometry analysis of CD62L and CD44 expression on splenic $CD4^+Foxp3^-$ and $CD8^+$ T cells of 6-month-old *Foxp3*^{Cre} and *Foxp3*^{Cre}*Wwtr1*$^{f/f}$ mice. (G) Flow cytometry analysis of YFP-Foxp3 expression in splenic $CD4^+$ T cells of *Foxp3*^{Cre} and *Foxp3*^{Cre}*Yap1*$^{f/f}$*Wwtr1*$^{f/f}$ mice. (H) Flow cytometry analysis of YFP-Foxp3 expression in splenic $CD4^+$ T cells of 6-month-old *Foxp3*^{Cre} and *Foxp3*^{Cre}*Yap1*$^{f/f}$ mice. (I) Flow cytometry analysis of YFP-Foxp3 expression in splenic $CD4^+$ T cells of 6-month-old *Foxp3*^{Cre} and *Foxp3*^{Cre}*Wwtr1*$^{f/f}$ mice. (J) Statistics of p-$STAT5^+$ population frequency in WT or Yap-deficient Tregs stimulated with IL-2 for 30 min. (K) Statistics of p-$STAT5^+$ population frequency in WT or Taz-deficient Tregs stimulated with IL-2 for 30 min. Numbers in quadrants or gates indicate percentage of cells. Data in plots indicate means ± s.e.m. Data are representative of 2 independent experiments (A–I) or pooled from 2 independent experiments (J, K).

Figure S7, related to Figures 6 and 7

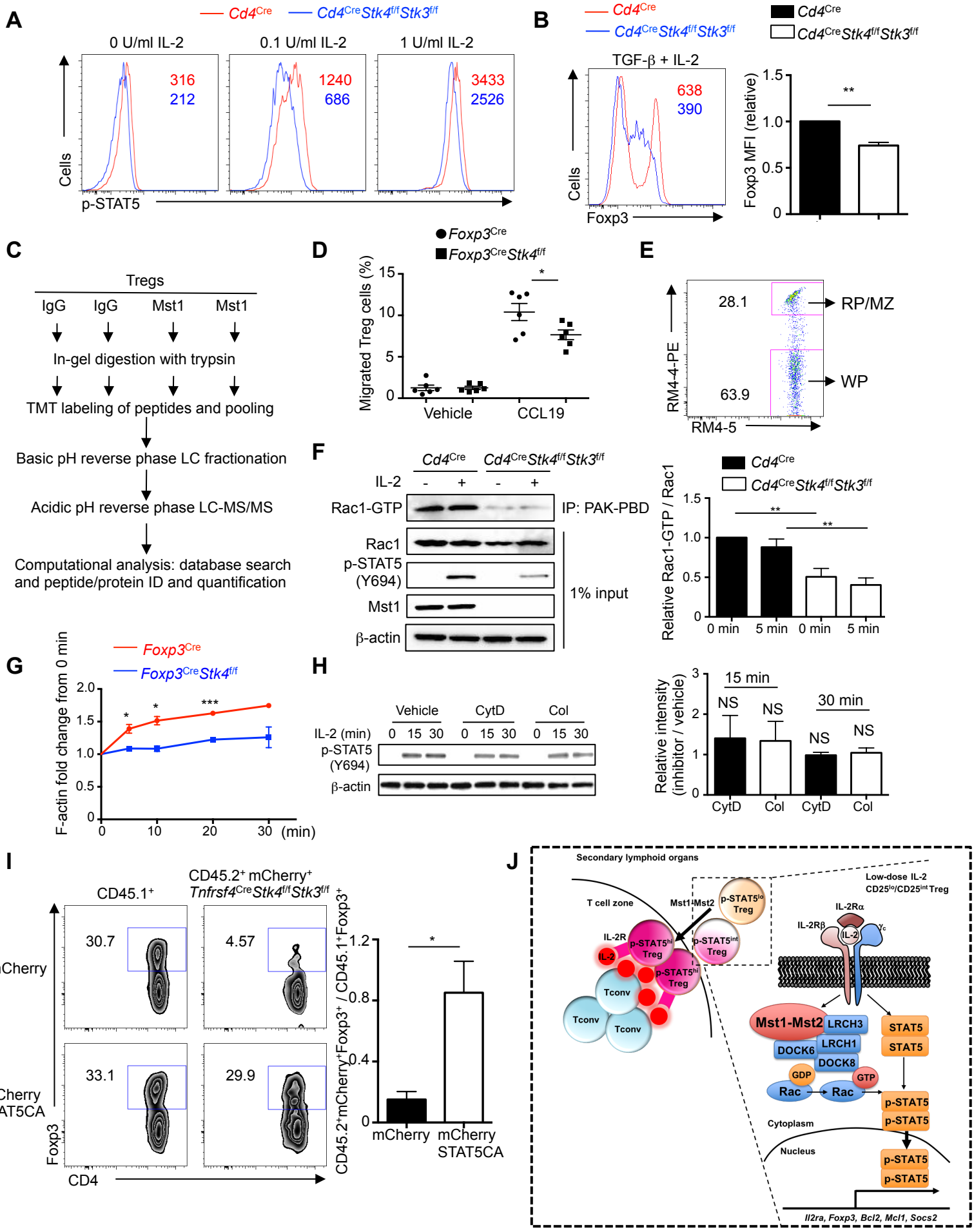

Figure S7, related to Figures 6 and 7. Mst1−Mst2 mediate Rac activation to interplay with IL-2–STAT5 signaling. (A) *In vitro*-derived Tregs from WT and *Cd4*^{Cre}*Stk4*$^{f/f}$*Stk3*$^{f/f}$ mice were rested without IL-2 for 4 h and re-stimulated with IL-2 for 30 min. p-STAT5 was analyzed by phosflow in Foxp3^{+} Tregs. (B) CD62L^{hi}CD69^{lo} mature thymocytes from WT and *Cd4*^{Cre}*Stk4*$^{f/f}$*Stk3*$^{f/f}$ mice were differentiated in Treg skewing condition for 5 days, and Foxp3 expression was examined by flow cytometry (left). Numbers in the graph indicate mean fluorescence intensity. Right, statistics of relative Foxp3 expression (n = 5) , with Foxp3 expression WT Tregs normalized to 1. (C) The flow chart of TMT-labeled quantitative interaction proteomics of endogenous Mst1 protein (alias: Stk4) in *in vitro* generated Tregs (duplicates in each group). (D) A million of total splenocytes from *Foxp3*^{Cre} and *Foxp3*^{Cre}*Stk4*$^{f/f}$ mice were loaded to the upper chamber of the 24-well transwell plate (n = 6), and vehicle or 200 ng/ml CCL19 containing RPMI 1640 medium was placed into the lower chamber. After 3 h incubation, the cells in lower and upper chambers were stained with CD4, CD8 and TCRβ followed by flow cytometry analysis. The ratio of YFP^{+} Tregs in lower chamber vs. total YFP^{+} Tregs loaded before incubation was calculated and compared between *Foxp3*^{Cre} and *Foxp3*^{Cre}*Stk4*$^{f/f}$ mice. (E) For *in vivo* T cell labeling, anti–CD4-PE antibody (RM4-4) was injected intravenously, and spleens were harvested 5 min after injection. Splenocytes were examined by flow cytometry after staining with the RM4-5 clone anti-CD4 antibody. A representative flow cytometry plot depicts the dual-labeled red pulp/marginal zone (RP/MZ) and single-labeled white pulp (WP) CD4^{+} Tregs. (F) *In vitro*-derived Tregs (CD4^{+}CD25^{hi}) from CD4^{+}CD62L^{hi}CD69^{lo} mature thymocytes of WT and *Cd4*^{Cre}*Stk4*$^{f/f}$*Stk3*$^{f/f}$ mice were starved in serum-free medium for 4 h and re-stimulated with IL-2 (100 U/ml) for 5 min. Rac1-GTP was immunoprecipitated by PAK-PBD beads, followed by immunoblot with Rac1 antibody to measure Rac1 activity (left). p-STAT5 (Y694) and Rac1 were also analyzed in the lysate (input). Right, statistics of seven experimental repeats of relative Rac1 activity (Rac1-GTP vs. Rac1), with WT Tregs at 0 min normalized to 1. (G) Fold changes of F-actin content in WT and Mst1-deficient Tregs (n = 3) upon IL-2 stimulation were quantified (value at 0 min was set to 1). (H) WT Tregs were pretreated with cytochalasin D (CytD; inhibitor of actin and microtubule reorganization) or colchicine (Col; inhibitor of microtubule reorganization) for 30 min, followed by stimulation with 1 U/ml IL-2. Immunoblot analysis of p-STAT5 was performed (n = 3 per treatment, left). Right, p-STAT5 in inhibitor vs. vehicle treated group was quantified. (I) Flow cytometry analysis of Foxp3^{+} Treg frequency in CD4^{+} T cells from CD45.2^{+}mCherry^{+} (mCherry or mCherry-STAT5CA) and CD45.1^{+} (spike) populations in retrogenic mice (generated by reconstituting *Rag1*$^{-/-}$ mice with *Tnfrsf4*^{Cre}*Stk4*$^{f/f}$*Stk3*$^{f/f}$ BM cells transduced with mCherry or mCherry-STAT5CA retrovirus, together with CD45.1^{+} BM cells to prevent autoimmunity) (left). Right, fold change of Foxp3^{+} Treg frequency of CD45.2^{+}mCherry^{+} (mCherry or mCherry-STAT5) vs. CD45.1^{+} population in retrogenic mice ($n \geq 4$). Numbers in gates indicate percentage of cells. Data in plots indicate means ± s.e.m. NS, not significant; *P < 0.05, **P < 0.01, ***P < 0.001; two-tailed unpaired Student's t test (B, D, G, H, I) or one-way ANOVA (F). Data are from 1 experiment (C) or representative of at least 2 independent experiments (A, B, E, F, H, I) or pooled from 2 independent experiments (D, G). (J) Schematics of Mst1−Mst2−Rac axis in mediating IL-2–STAT5 signaling in Tregs. Mst1 promotes Treg access to the IL-2 source produced by conventional T cells (Tconv) in the T cell zone of secondary lymphoid organs as a cell-extrinsic mechanism. For cell-intrinsic mechanism, Mst1−Mst2 couple with CD25 to adapt Tregs to a low IL-2 threshold. In IL-2 limited condition or Tregs with low CD25 expression, Mst1−Mst2 signaling takes effect by regulating Rac activity through interacting with GTPase DOCK8−LRCHs module (containing LRCH1, LRCH3, DOCK6 and DOCK8 proteins). Rac activation in turn promotes STAT5 phosphorylation, thereby amplifying IL-2–STAT5 signaling in Tregs to maintain survival and lineage stability. Targeting Mst1−Mst2−Rac axis could potentially modulate Treg responses to low-dose IL-2 and provides opportunities for therapeutic intervention of autoimmunity and other immune-mediated diseases.

Kinase inhibitor	Target	Working concentration	Vendor	p-STAT5 inhibition (%) at IL-2 30 min
XMU-MP-1	Mst1	5 μM	Selleck Chemicals	48.2
Tofacitinib	JAK3	1 μM	Tocris	87.3
PS-1145	IKKβ	10 μM	Cayman Chemical	1.4
U-0126	ERK	10 μM	Cayman Chemical	1.5
SB203580	p38 MAPK	20 μM	EMD Millipore	0
GSK2334470	PDK1	10 μM	EMD Millipore	6.4
Akt inhibitor VIII	AKT	1 μM	EMD Millipore	0
Rapamycin	mTORC1	50 nM	EMD Millipore	2.3
SP600125	JNK	10 μM	Sigma-Aldrich	0
LY294002	PI3K	10 μM	Sigma-Aldrich	0
SB216763	GSK3	10 μM	Tocris	0
MK2 inhibitor	MK2	5 μg/ml	Tocris	0
MNK1 inhibitor	MNK1	20 μM	EMD Millipore	0
MSK1 inhibitor	MSK1	20 μM	Tocris	0

Table S1, related to Figure 1. Effects of kinase inhibitors on IL-2-induced p-STAT5 in Tregs. $CD4^+CD25^+$ Tregs were pretreated with vehicle or the kinase inhibitors in the table at indicated working concentrations for 30 min at 37ºC, and then stimulated with IL-2 (5 U/ml) for 30 min for p-STAT5 phosflow analysis to obtain mean fluorescence intensity. Drug inhibition (%) was calculated as: (Vehicle – Inhibitor) / Vehicle × 100%. p-STAT5 level equal or higher than the vehicle control was considered as no inhibition (0%). The data are representative of 3 independent experiments.